



Heterogeneous photodegradation of pentachlorophenol and iron cycling with goethite, hematite and oxalate under UVA illumination

Qing Lan^{a,b,d}, Fang-bai Li^{b,*}, Cui-xiang Sun^b, Cheng-shuai Liu^b, Xiang-zhong Li^c

^a Guangzhou Institute of Geochemistry, Chinese Academy of Sciences, Guangzhou 510640, PR China

^b Guangdong Key Laboratory of Agricultural Environment Pollution Integrated Control, Guangdong Institute of Eco-Environmental and Soil Sciences, Guangzhou 510650, PR China

^c Department of Civil and Structural Engineering, The Hong Kong Polytechnic University, Hong Kong, PR China

^d Graduate University of Chinese Academy of Sciences, Beijing 100039, PR China

ARTICLE INFO

Article history:

Received 6 December 2008

Received in revised form 3 September 2009

Accepted 6 September 2009

Available online 11 September 2009

Keywords:

Heterogeneous photodegradation

Pentachlorophenol

Iron cycle

Goethite

Hematite

Oxalate

ABSTRACT

Heterogeneous photodegradation of pentachlorophenol (PCP) in the goethite (α -FeOOH) and hematite (α -Fe₂O₃) systems with oxalate under UVA illumination was investigated. The PCP degradation, dechlorination and detoxification, in terms of Microtox acute toxicity, were all achieved to the higher efficiency in the hematite suspension than in the goethite suspension. The optimal initial concentration of oxalic acid (C_{ox}^0) for the PCP degradation with goethite and hematite under the experimental conditions was found to be 1.2 mM, since sufficient Fe(III) as Fe(C₂O₄)₃³⁻ and Fe(II) as Fe(C₂O₄)₂²⁻ can be formed at $C_{ox}^0 \geq 1.2$ mM. The main intermediates of PCP degradation were identified by GC-MS, HPLC and IC analyses. It was found that the cycling process between Fe(III) and Fe(II) in both the goethite and hematite systems occurred more vigorously at the initial stage and gradually became gentle, while the rate of PCP photodegradation varied from fast to slow during the reaction time. Furthermore, the formation of H₂O₂ during photoreaction was studied to explore its relationship with the photodegradation efficiency and the iron cycling process.

© 2009 Elsevier B.V. All rights reserved.

1. Introduction

Iron, as the fourth most abundant element of the earth's crust, is rich in the environment. Oxalic acid, mainly secreted by plant roots [1] or formed by incomplete combustion of hydrocarbons [2,3], is ubiquitous in soil, water and atmosphere. In nature, iron, oxalic acid and sunlight can establish a homogeneous photo-Fenton-like system where iron exists in a dissolved form, or a heterogeneous photo-Fenton-like system where iron is in a solid form. The heterogeneous Fe(III)-oxalate system should be more applicable to the natural environment, because the iron species are mostly present as amorphous or (hydr)oxides. In the 1990s several research groups [4–8] studied the mechanisms of iron (hydr)oxides dissolution in aqueous oxalate solution. Sulzberger's group explored the degradation of diuron in a goethite-oxalate system irradiated by UV [9]. Our group studied the effects of reaction conditions and the distribution of various iron species in the iron oxide-oxalate-UV system [10–13]. It is generally accepted that the reaction mechanisms of such a heterogeneous system include several critical processes. The chemical adsorption of oxalic acid first occurs on the surface of iron oxide leading to the formation of Fe-oxalate complexes,

and simultaneously the non-reductive/reductive dissolution of iron oxide takes place [9–13]. Light irradiation can greatly enhance the reductive dissolution of Fe(III)-oxalate complexes, yielding Fe(II) and oxalate radical (C₂O₄)^{•-} [6–13]. In the presence of O₂, the most reactive oxidant, •OH, can be obtained by the Fenton reaction of H₂O₂ with Fe(II), and iron cycling involving a series of active radicals can take place in the system [2,3,13–15].

Compared with the classical photo-Fenton systems (Fe²⁺ or Fe³⁺/H₂O₂), the photo-Fe-oxalate system can form H₂O₂ in situ, and has the higher efficiency for the degradation of organic compounds [1,14,16]. While the homogeneous Fe-oxalate systems have been explored in many previous studies [1–3,14–20], the heterogeneous Fe-oxalate systems, which do not easily bring about the secondary contamination of abundant dissolved Fe ions in practical applications, have only received scant attention.

In the heterogeneous system, various iron (hydr)oxides demonstrate different dissolution properties [8]. The preparation method and intrinsic structure largely influence the activities of iron oxides [21–23]. Doping agents also significantly affect the photocatalytic activity of iron oxides [24,25]. In the irradiated heterogeneous iron oxide-oxalate system, iron cycling, which happens both heterogeneously and homogeneously [6–8,10], is essential because it produces H₂O₂ and •OH continuously. However, studies of the dissimilarities of iron oxides with different crystal structures in degrading contaminants and especially the generation of H₂O₂ and

* Corresponding author. Tel.: +86 20 87024721; fax: +86 20 87024123.
E-mail addresses: cefbli@soil.gd.cn, cefbli@hotmail.com (F.-b. Li).

the different Fe species are scant, but are very important for understanding such complicated heterogeneous reactions.

In the present study, pentachlorophenol (PCP) was chosen as a probe pollutant because of its persistence in the environment and high toxicity due to the five chlorine atoms in its structure. The aim was at comparing the activities of two iron oxides (goethite and hematite) in degrading PCP with oxalate under UV illumination, and investigating the formation of H_2O_2 , and the adsorbed/dissolved Fe species cycling. In addition, the dechlorination, detoxification (Microtox acute toxicity) and intermediates of PCP were investigated.

2. Experiments and methods

2.1. Chemicals

PCP (98%) was purchased from Aldrich, USA. Tetrachloro-*p*-benzoquinone (99%), tetrachloro-*o*-benzoquinone (97%), methanol (HPLC grade) and hexane (HPLC grade) were obtained from Acros, Belgium. Other chemicals with analytical grade were purchased from Guangzhou Chemical Co. China. All the chemicals were used as received except acetic anhydride, which was redistilled for GC/MS analysis. Deionized water (18.2 m Ω .cm) from an ultrapure water system (Easy Pure^{II} RF/UV, USA) was used in all experiments. Goethite (α -FeOOH) and hematite (α -Fe₂O₃) powders were synthesized according to the procedures previously reported [26]. While their composition and crystal structures were confirmed by X-ray powder diffraction (XRD), their specific surface areas were measured to be 32.3 and 29.4 m² g⁻¹, respectively by the Brunauer–Emmett–Teller (BET) method.

2.2. Photochemical experiment

Aqueous PCP stock solution (0.075 mM) was prepared with 1.0% (v/v) ethanol and stored in a dark-brown glass bottle to avoid any photochemical reaction. In all photodegradation experiments, aqueous suspensions contained the same initial PCP concentration (0.0375 mM) and the same iron oxide content (0.4 g L⁻¹), but different initial concentrations of oxalic acid (C_{ox}^0). Ethanol was used to prepare the above aqueous PCP solutions and its concentration in all experiments was kept strictly at 0.5% as it is an $\cdot\text{OH}$ scavenger. It is believed that the ethanol would affect PCP degradation to a similar extent in all experiments, but should not affect the pattern of PCP degradation kinetics. All experiments were carried out in a photochemical reactor system described in detail previously [10]. The experiments were performed at 30 °C using a thermostatted water bath. Prior to UV light irradiation, adsorption/desorption equilibrium in the aqueous PCP suspension was established in the dark for 30 min. The suspension was continuously stirred by a magnetic stirrer and bubbled with air throughout each experiment. The water samples for HPLC, IC and GC–MS analyses were taken at various time intervals and then were centrifuged at 4500 rpm for 25 min, and further filtered through a 0.45 μm filter before injecting into the analytical instruments. The initial pH of suspensions was adjusted to 3.5 using NaOH or HClO₄ solution.

2.3. Analysis

PCP and some intermediates were determined by HPLC (Waters 1525/2487) with an Xterra C18 reverse-phase column. For PCP analysis, a mobile phase containing 1% acetic acid in water/methanol (20:80, v/v) mixed solvent flew at a rate of 1.0 mL min⁻¹. The column temperature was set at 35 °C and UV detection was set at 295 nm. Following the analytical procedure described by

Oturan et al. [27], tetrachloro-*p*-benzoquinone and tetrachloro-*o*-benzoquinone were identified by comparing their retention times in HPLC with internal standards. The mobile phase and flow rate were the same as noted above, but the ratio of 1% acetic acid in water to methanol was 25:75 (v/v), and the column temperature and the detector wavelength were set at 30 °C and 280 nm, respectively.

The concentrations of oxalic acid and chloride ions were determined by ion chromatography (IC Dionex ICS-90) with a mobile phase of aqueous 1.0 mM NaHCO₃–8.0 mM Na₂CO₃ solution at a flow rate of 1.0 mL min⁻¹. An LC-10A system (Shimadzu) with IC-A3 column was used to identify the intermediate products (HCOOH and CH₃COOH) with a mobile phase of 2.5 mM phthalic acid and 2.4 mM Tris solution at a flow rate of 1.2 mL min⁻¹ and 40 °C.

H₂O₂ in aqueous solution was measured using an H₂O₂ analyzer (Lovibond-ET8600, Germany), in which Lovibond reagent was reacted with H₂O₂ in a 10 mL vessel to form a colored solution, and the concentration of H₂O₂ was determined photometrically at 528 nm with a detection limit of 0.05 mg L⁻¹. The Lovibond reagent was first added in the vessel before the sample was taken from the photoreactor. At each time interval, 10 mL of reaction solution was sampled and immediately filtered through a 0.45 μm filter before it was placed into the vessel, and the concentration of H₂O₂ in the filtrate was measured at once. As this procedure was completed within 1 min, the validity of H₂O₂ concentration was ensured.

A GC–MS (Thermo Trace-DSQ-2000) system with electron ionization and an Agilent silicon capillary column (0.25 mm \times 30 m) was used to determine other products from PCP degradation in which the samples were pretreated by extraction as the described previously [28,29].

A Microtox analyzer (Strategic Diagnostics Inc., U.S. Model 500) was used to measure the Microtox acute toxicity of samples, in which the relative degree of sample toxicity is expressed by the percentage of light loss. The details of the measurement method can be found elsewhere [13].

Dissolved Fe(II) was measured colorimetrically by the ferrozine method and total dissolved iron was determined in the same way after adding 10% OHNH₃Cl to reduce all Fe(III)(aq) to Fe(II)(aq). The adsorbed Fe(III)/Fe(II) on the surface of iron oxide was extracted by 0.1 M HCl solution with stirring for 30 min in the dark prior to the above analyses. Since no iron ion was detected in the α -FeOOH/ α -Fe₂O₃ suspensions in the absence of oxalic acid under this extraction condition, it indicated that the fixed iron of α -FeOOH/ α -Fe₂O₃ should not be extracted to interfere with the measurement of adsorbed Fe species. To avoid the oxidation of Fe(II), the sample filtered through the 0.45 μm filter was measured promptly after sample collection. In the measurement of Fe(III), several minutes were needed to allow complete reduction of Fe(III) to take place before addition of the buffer and ferrozine.

3. Results and discussion

3.1. Photodegradation of PCP

The experimental results of PCP photodegradation under different conditions are presented in Fig. 1. The results showed that 30–68% of PCP was removed after 1 h reaction time in the α -FeOOH suspension with different initial concentrations of oxalic acid (C_{ox}^0) (Fig. 1A), which was much lower than that (49–83%) in the α -Fe₂O₃ suspension (Fig. 1B). In the absence of oxalic acid, PCP was only slightly degraded by direct photolysis at below 370 nm [28]. The results demonstrate that the presence of oxalic acid greatly enhanced PCP degradation and an optimal C_{ox}^0 in the α -FeOOH and α -Fe₂O₃ systems was found to be around 1.2 mM. With this optimal C_{ox}^0 , 68% and 83% of PCP was photocatalytically degraded after 1 h in the α -FeOOH and α -Fe₂O₃ systems, respectively.

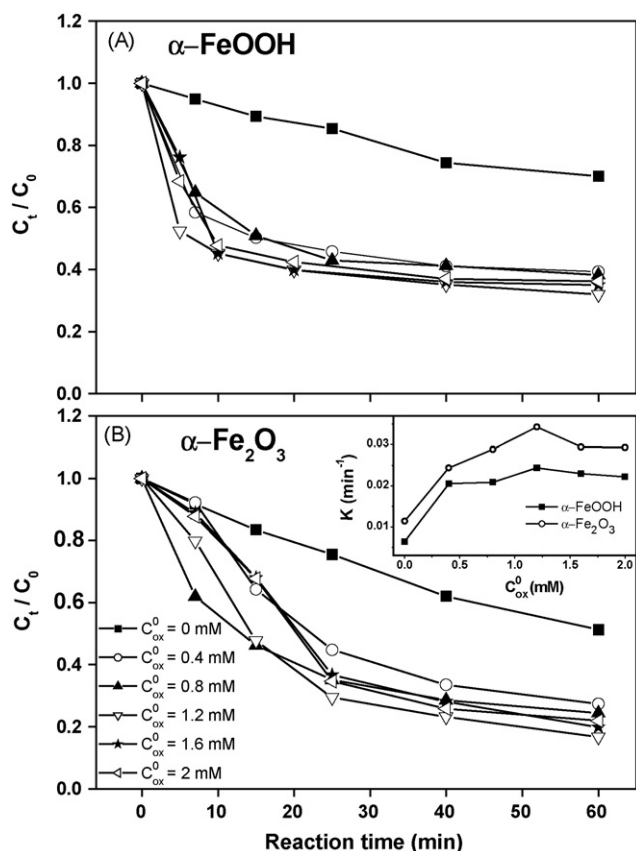


Fig. 1. The photodegradation of PCP versus reaction time in the irradiated heterogeneous systems with 0.4 g L^{-1} iron oxides and different C_{ox}^0 at initial pH 3.5: (A) α -FeOOH suspension; (B) α -Fe₂O₃ suspension. The inserted plot shows the dependence of the first-order rate constant (k) of PCP degradation on C_{ox}^0 .

The Fe species should play an important role in the PCP degradation because various Fe species have different photoactivity [1,9,18]. For example, Fe(III) in the form of $\text{Fe}(\text{C}_2\text{O}_4)_2^-$ and $\text{Fe}(\text{C}_2\text{O}_4)_3^{3-}$ can be more efficiently photolyzed to Fe(II) than as other species [1,9,19], and Fe(II) as $\text{Fe}(\text{C}_2\text{O}_4)_2^{2-}$ can react with H_2O_2 to form $\cdot\text{OH}$ at a much faster rate than that as Fe^{2+} [1,9,19]. According to the method described by Panyas et al. [4], the fractions of different Fe species in iron oxide-oxalate suspensions can be calculated as the functions of pH and oxalic acid concentration. Using the tested pH values and oxalic acid concentrations during the experiments, the changes in distribution of different Fe(III)/Fe(II) species during the reaction time in the α -FeOOH or α -Fe₂O₃ suspension were calculated accordingly [13]. In the α -FeOOH or α -Fe₂O₃ suspension during the photoreaction, the Fe(III) species $\text{Fe}(\text{C}_2\text{O}_4)_2^-$ and/or $\text{Fe}(\text{C}_2\text{O}_4)_3^{3-}$ with high photoactivity were found to be the dominant species (>90%) at different C_{ox}^0 . For Fe(II) species in the two suspensions, it was found that at $C_{ox}^0 = 0.4$ mM, the Fe^{2+} species with low photoactivity was the dominant species (>60%). At $0.4 \text{ mM} < C_{ox}^0 < 1.2 \text{ mM}$, the amounts of Fe^{2+} and $\text{Fe}(\text{C}_2\text{O}_4)_2^{2-}$ were similar with a total Fe(II) species fraction of >90%, and at $C_{ox}^0 \geq 1.2$ mM, $\text{Fe}(\text{C}_2\text{O}_4)_2^{2-}$ became the dominant Fe(II) species (>80%). Consequently, it is reasonable to assume that at $C_{ox}^0 = 1.2$ mM in the α -FeOOH or α -Fe₂O₃ suspension, the two species of Fe(III) as $\text{Fe}(\text{C}_2\text{O}_4)_3^{3-}$ and Fe(II) as $\text{Fe}(\text{C}_2\text{O}_4)_2^{2-}$ with high photoactivity were formed to a sufficient extent to cause PCP degradation. However, since oxalic acid itself was also a scavenger of $\cdot\text{OH}$, the reaction rate of PCP degradation decreased at $C_{ox}^0 > 1.2$ mM.

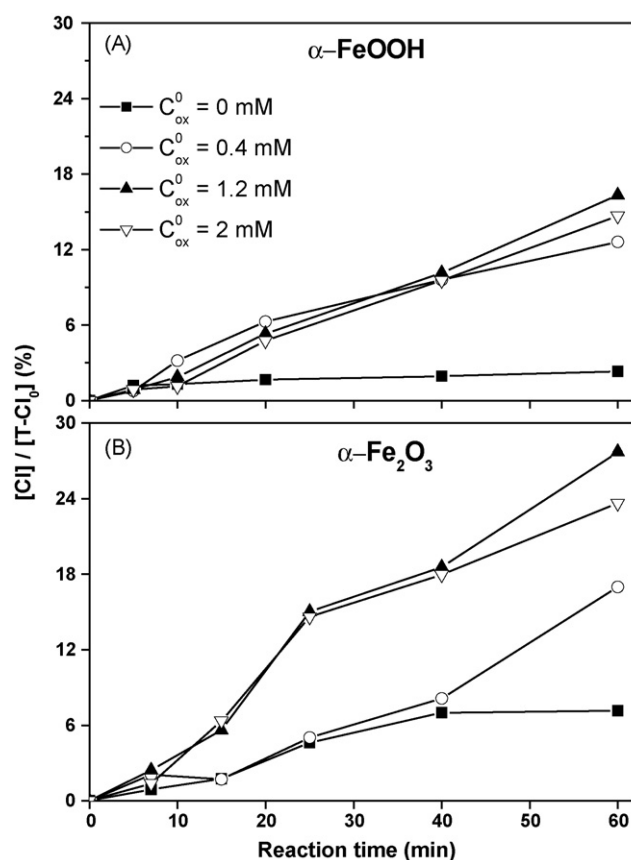


Fig. 2. The changes of dechlorination during PCP photodegradation in the irradiated heterogeneous systems with 0.4 g L^{-1} iron oxides and different C_{ox}^0 at initial pH 3.5: (A) α -FeOOH suspension; (B) α -Fe₂O₃ suspension.

3.2. Dechlorination and detoxification of PCP

The ratio of dechlorination (%) was calculated as $[\text{Cl}^-]/[\text{T-Cl}_0]$ where $[\text{Cl}^-]$ is the concentration of chloride released from PCP degradation and $[\text{T-Cl}_0]$ is the stoichiometric concentration of organic chlorine in PCP. Fig. 2 shows the rates of dechlorination in the two iron oxide systems with oxalate under UVA illumination. After 1 h reaction time, the dechlorination in the α -FeOOH system was achieved by 2–16% (Fig. 2A), which was much lower than that in the α -Fe₂O₃ system (7–28%) (Fig. 2B). The amount of released chloride was much higher in the presence than in the absence of oxalic acid. The highest rate of dechlorination was obtained at the optimal C_{ox}^0 of 1.2 mM in both the α -FeOOH and α -Fe₂O₃ suspensions. Furthermore, as described previously [13] the dechlorination reaction continued in the reactions with intermediate products after 1 h reaction time (data not shown here). Oturan et al. reported a similar phenomenon for PCP degradation in an electro-Fenton system [27]. These results may indicate that the cleavage of Cl–C bonds due to $\cdot\text{OH}$ attack has no preference compared to other degradation reactions in the system.

The data in Fig. 3 confirmed the detoxification of PCP in terms of light loss determined with the Microtox analysis. At $C_{ox}^0 = 1.2$ mM, the ratios of light loss after 1 h reaction decreased from 83% and 84% for the α -FeOOH and α -Fe₂O₃ systems to 54% and 46%, respectively. It is also proposed that the detoxification reaction continued with extension of the reaction time beyond 1 h as reported previously [13]. In addition, it is apparent that the results of dechlorination and detoxification were in line with the PCP degradation, indicating that PCP was degraded more efficiently in the α -Fe₂O₃ system than in the α -FeOOH system.

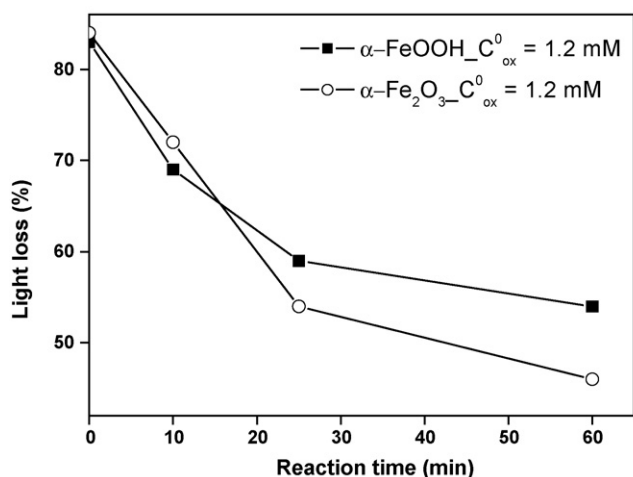


Fig. 3. Detoxification of PCP during the reaction time at the optimal C_{ox}^0 (1.2 mM) in the α -FeOOH and α -Fe₂O₃ systems under UVA illumination.

3.3. Intermediates from PCP degradation

Although PCP was degraded in the α -FeOOH and α -Fe₂O₃ systems at different rates, the same intermediates were identified in the two systems with oxalic acid under UVA illumination, including tetrachlorocatechol (TeCC) and 2,3,5,6-tetrachloro-1,4-hydroquinone (TeCHQ) by GC-MS, tetrachloro-*o*-benzoquinone (*o*-chloranil) and tetrachloro-*p*-benzoquinone (*p*-chloranil) by HPLC, and HCOOH and CH₃COOH by IC.

Hydroquinone has been found to catalyze the Fenton reaction because it can rapidly reduce Fe(III) to Fe(II), and lead to an intermediate cycling by generation of semiquinone products [30,31]. During the intermediate cycling, hydroquinone reduces Fe(III) to form semiquinone and the semiquinone reduces Fe(III) to form quinone, while hydroquinone and quinone can be renewably formed by the dismutation of semiquinone [30,31]. Such a intermediate cycling involving the reduction of Fe(III) can combine with the iron cycling of the system to accelerate the generation of Fe(II) and active species [31]. The intermediate cycling is described by equations (1)–(4), and the results in Section 3.5 showed that more H₂O₂ was formed in the presence than in the absence of PCP, indicating the existence of the intermediate promotion mechanism involving the iron cycling.

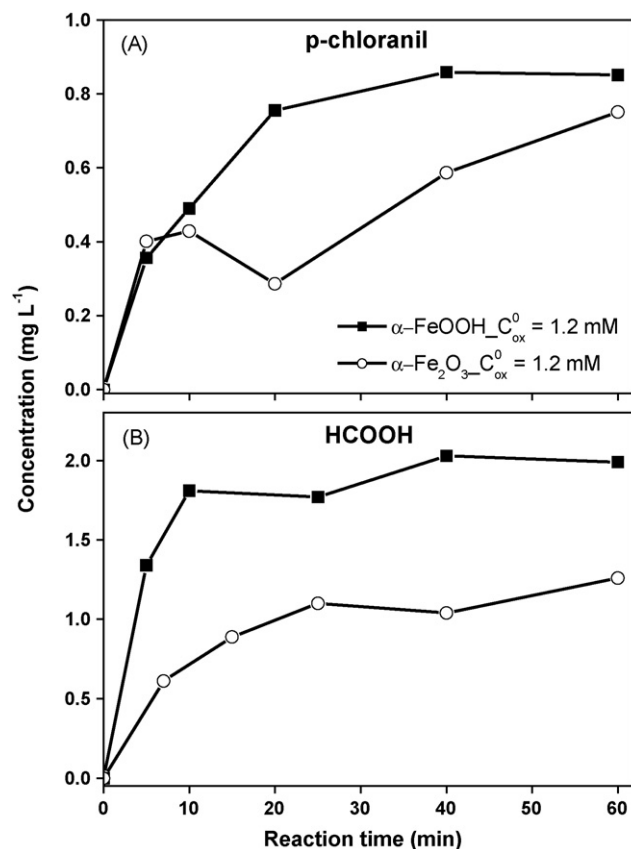
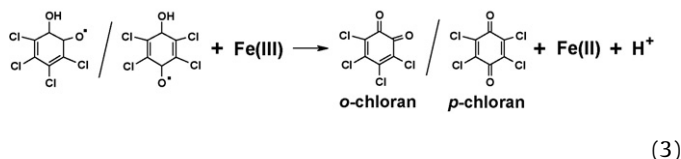
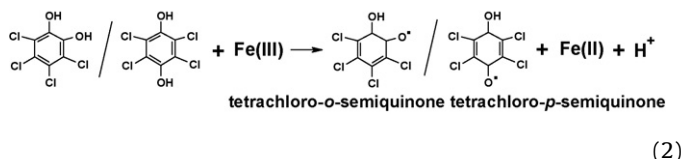
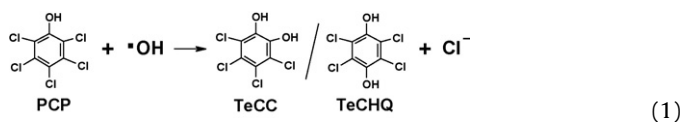
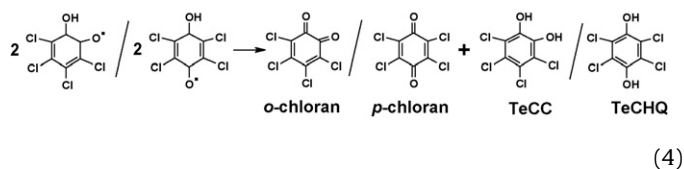


Fig. 4. Concentration changes of PCP intermediates versus reaction time at the optimal C_{ox}^0 (1.2 mM) in the α -FeOOH and α -Fe₂O₃ systems under UVA illumination. (A) *p*-chloranil; (B) HCOOH.



The above intermediate cycling can explain to some extent why production of Cl₃C₆(OH)₃ was not detected, because the oxidation to tetrachloro benzoquinone is more favorable compared with further hydroxylation of the ring in such systems. Augusti et al. [32] reported similar results for chlorobenzenes degradation by Fenton's reagent. The formation of organic acids with small molecules such as HCOOH and CH₃COOH confirmed that PCP was mineralized to some extent after its aromatic ring was broken after 1 h reaction time.

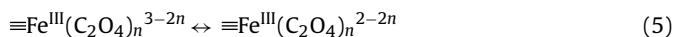
The control experiments showed that CH₃COOH was formed by oxidation of PCP and/or ethanol. Since the formation and degradation of intermediates occurred at the same time, and the hydroquinone products of PCP could accelerate the reaction, it was difficult to quantify the contribution of PCP to the fraction of CH₃COOH formation. Two other intermediates, tetrachloro-*p*-benzoquinone (*p*-chloranil) and HCOOH, were quantified as shown in Fig. 4. It was found that the concentrations of the two intermediates were significantly higher in the α -FeOOH system than in the α -Fe₂O₃ system. The results in Sections 3.1 and 3.5 showed that the both rates of PCP degradation and H₂O₂ formation were significantly lower in the α -FeOOH suspension than in the α -Fe₂O₃ suspension. All of these results indicated that more active substances could be generated in the α -Fe₂O₃ suspension to degrade

the intermediates from PCP degradation. The shorter lifetime of these intermediates resulted in less accumulation in the α -Fe₂O₃ suspension.

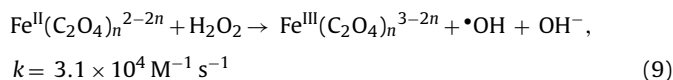
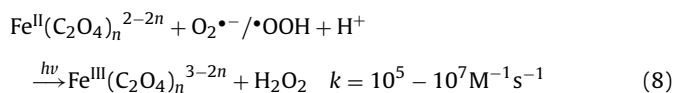
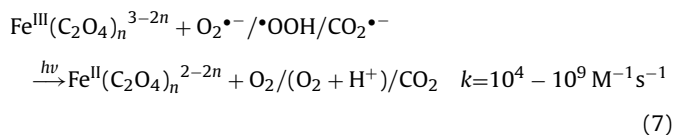
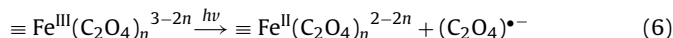
3.4. Iron cycling during PCP degradation

Iron cycling is a key step in the Fenton reaction to continuously form H₂O₂ and •OH in an iron oxide-oxalate system, either in the dark or under light irradiation, as shown below [4–8]:

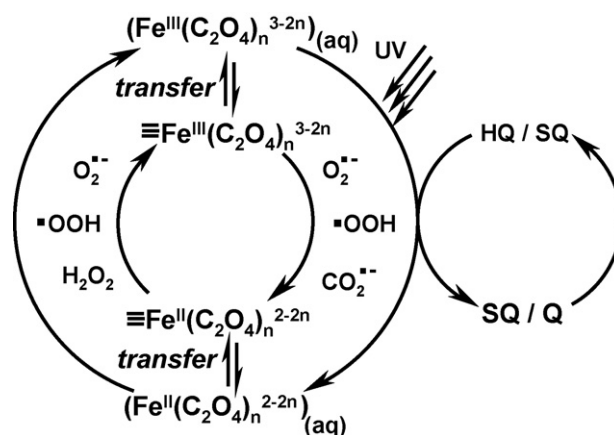
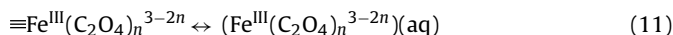
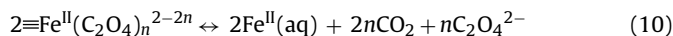
In the dark: [5]



Under light irradiation: [1,16,33,34]



In addition, the interface transfer process should be involved throughout the iron cycling: [33]



Scheme 1. The mechanism of iron cycling with iron oxides and oxalate under UVA illumination in the presence of PCP. HQ and Q represent the hydroquinone (TeCC/TeCHQ) and quinone (*o*-chloranil/*p*-chloranil) intermediates detected. SQ represents the tetrachloro-*o*-semiquinone/tetrachloro-*p*-semiquinone radicals.

The mechanism of iron cycling in the iron oxide-oxalate-UV system in the presence of PCP is presented in Scheme 1. This cycling takes place simultaneously both on the surface of iron oxide and in the bulk solution. The hydroquinone/quinone intermediates of PCP can catalyze this cycling as discussed above (Eqs. (1)–(4)). The interface transfer processes (Eqs. (10) and (11)) of Fe(III)/Fe(II) play an important role in the interaction between surface reaction and solution reaction.

To quantitatively study the iron cycling during PCP degradation, the concentrations of adsorbed and dissolved Fe(III)/Fe(II) versus reaction time were determined as shown in Fig. 5. The concentration of adsorbed/dissolved Fe(III)/Fe(II) was mainly in the range 0.01–0.10 mM, which was much lower than the stoichiometric concentration corresponding to 0.4 g L⁻¹ of α -FeOOH/ α -Fe₂O₃ and the initial concentration of oxalic acid used. However, Zuo and Hoigne [2,3] reported that H₂O₂ and •OH could be formed at much lower concentrations of Fe(III) (1 μ M) and oxalate (5 μ M), indicating that

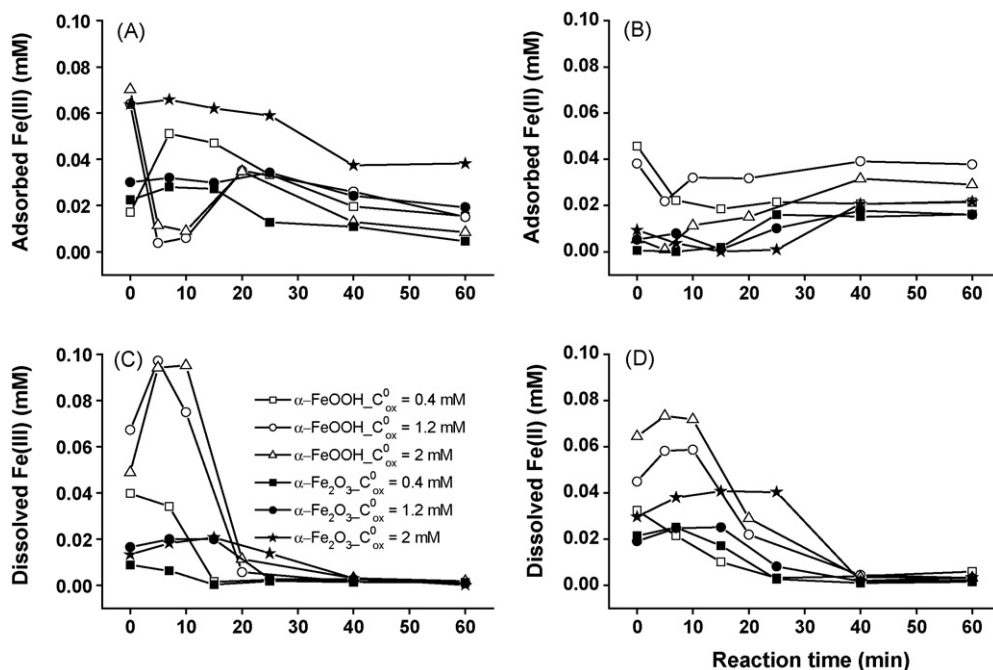


Fig. 5. The concentration variation of adsorbed/dissolved Fe during PCP photodegradation at different C_{ox}^0 in the α -FeOOH and α -Fe₂O₃ systems. (A) the adsorbed Fe(III); (B) the adsorbed Fe(II); (C) the dissolved Fe(III); (D) the dissolved Fe(II).

the amounts of Fe(III)/Fe(II) in our experiments were sufficient to form H_2O_2 and $\bullet\text{OH}$.

After 30 min of adsorption/desorption equilibration in the dark, the concentration of adsorbed Fe(III) increased with the increase of C_{ox}^0 in both the $\alpha\text{-FeOOH}$ and $\alpha\text{-Fe}_2\text{O}_3$ systems. Only small amounts of dissolved Fe(III) and Fe(II) were formed by desorption of surface Fe(III)-oxalate complexes (Eq. (11)) and the slow reductive dissolution in the dark (Eq. (5)).

Fig. 5 indicates that the amounts of all Fe species during photodegradation of PCP varied greatly in the initial stages of reaction, which might result from the fast redox cycling of Fe(III)/Fe(II) with vigorous interface transfer. It is known that light irradiation can greatly enhance the photochemical electron transfer of Fe(III)-oxalate complexes (Eqs. (6)–(9)) [5–8]. In the late stage of reaction, the variation of the amounts of the different Fe species declined significantly, which might result from the loss of oxalic acid and the increase of pH. Correspondingly, as shown in Fig. 1, the degradation of PCP in the $\alpha\text{-FeOOH}$ or $\alpha\text{-Fe}_2\text{O}_3$ suspension had the same pattern of rapid degradation in the initial stage and gradually decreasing degradation rate in the later stage.

In the study [35], different iron oxides with almost the same concentration of total dissolved Fe showed different activities towards degradation of mordant yellow 10 (MY 10) in the iron oxide- H_2O_2 suspension. In this study, it was found that the concentrations of dissolved Fe(III)/Fe(II) were higher in the $\alpha\text{-FeOOH}$ system than in the $\alpha\text{-Fe}_2\text{O}_3$ system during the reaction time as shown in Fig. 5. However, PCP degradation was slower in the $\alpha\text{-FeOOH}$ system than in the $\alpha\text{-Fe}_2\text{O}_3$ system. These results indicated that the amount of dissolved iron is not a rate-determining factor in relation to the activity of the iron oxides with different crystal structures. The exact mechanisms determining the activity of different iron oxides may involve their specific surface characters and the specific properties of target pollutants that need to be explored in further research.

In these heterogeneous iron oxide-oxalate systems, the dissolved Fe(II)/Fe(III) resulted from the redox reaction of Fe(III)/Fe(II) in solution, and also the interface transfer of Fe(II)/Fe(III) on the surface. As shown in Fig. 5, it is interesting that the amounts of adsorbed Fe(II)/Fe(III) in the $\alpha\text{-FeOOH}$ or $\alpha\text{-Fe}_2\text{O}_3$ system remained almost constant during the late stage of reaction, indicating that the interface transfer process of Fe(II)/Fe(III) from surface to solution became slow due to the consumption of oxalic acid with the increase of pH, and might be a relatively slow process during the iron cycling. Sulzberger and co-workers [8,9] and Banwart et al. [36] noted that the interface process of detachment of Fe(II) from the surface was the rate-determining step in an iron oxide-oxalate-UV system [8,9,36]. The results of this study should provide useful information to better understand the role of the interface transfer process during iron cycling in such heterogeneous systems.

3.5. Formation of hydrogen peroxide

The most reactive oxidant, $\bullet\text{OH}$, is obtained through the H_2O_2 reaction with Fe(II), while H_2O_2 is mainly generated by the reaction of Fe(II) with $\text{O}_2 \cdot \bullet/\bullet\text{OOH}$ and the dismutation of $\text{O}_2 \cdot \bullet/\bullet\text{OOH}$ in the presence of O_2 [1–3]. The concentration of H_2O_2 in the system depends on both the rates of its generation and consumption. The more rapid is iron cycling, the greater amount of H_2O_2 can be formed. The variation of H_2O_2 concentration versus reaction time in the $\alpha\text{-FeOOH}$ and $\alpha\text{-Fe}_2\text{O}_3$ suspensions is presented in Fig. 6.

In the absence of oxalic acid, H_2O_2 was not detected during 60 min in the $\alpha\text{-FeOOH}$ or $\alpha\text{-Fe}_2\text{O}_3$ system. In the presence of oxalic acid, H_2O_2 was detected at a significant level between 0.1 and 1.2 mg L^{-1} in the $\alpha\text{-FeOOH}$ suspension (Fig. 6A) and 1.2 and 3.0 mg L^{-1} in the $\alpha\text{-Fe}_2\text{O}_3$ suspension (Fig. 6B). In both the $\alpha\text{-FeOOH}$ and $\alpha\text{-Fe}_2\text{O}_3$ systems, more H_2O_2 could be formed in the presence

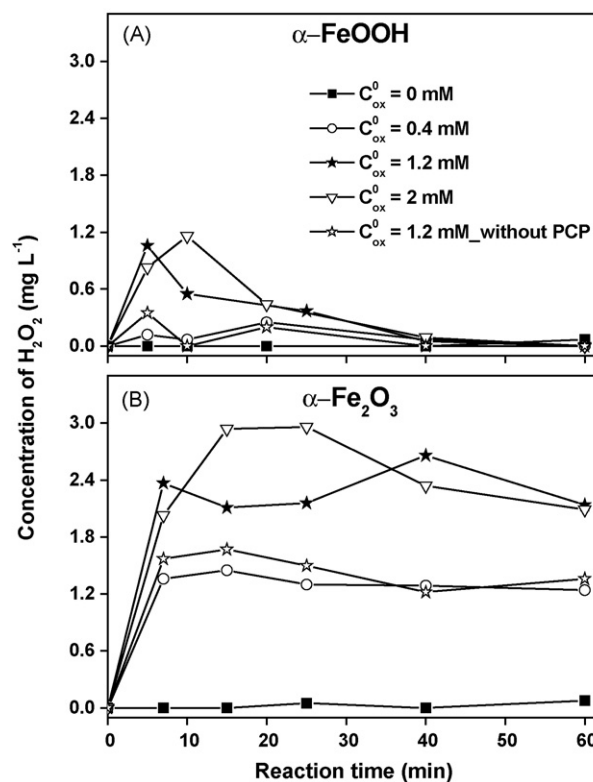


Fig. 6. The formation of H_2O_2 during PCP degradation in the irradiated heterogeneous system with 0.4 g L^{-1} iron oxides and different C_{ox}^0 at initial pH 3.5. (A) $\alpha\text{-FeOOH}$ system; (B) $\alpha\text{-Fe}_2\text{O}_3$ system.

than in the absence of PCP at $C_{\text{ox}}^0 = 1.2 \text{ mM}$, and the concentrations of H_2O_2 at $C_{\text{ox}}^0 \geq 1.2 \text{ mM}$ were much higher than at $C_{\text{ox}}^0 = 0.4 \text{ mM}$. It was apparent that the concentration of H_2O_2 was significantly higher in the $\alpha\text{-Fe}_2\text{O}_3$ system than in the $\alpha\text{-FeOOH}$ system.

The above results may explain why PCP was more effectively photodegraded in the $\alpha\text{-Fe}_2\text{O}_3$ system. In addition, the above results to a certain extent confirmed that the hydroquinone intermediates could accelerate iron cycling and promote the formation of active compounds as discussed in Sections 3.3 and 3.4.

The Fe(III)-oxalate complexes are initially formed by the adsorption of oxalic acid [9,13]. Then the photo-reduction of Fe(III)-oxalate complexes can generate H_2O_2 and a series of active radicals [1–3]. Thus, the amount of oxalic acid adsorption on the surface of iron oxide directly influenced the formation of H_2O_2 . However, the adsorption abilities of different iron oxides are different due to different surface properties and crystal structures.

Recently, we systematically studied the adsorption behavior of oxalic acid on the surface of different iron oxides, including some important effect factors. It was found that the ability of $\alpha\text{-Fe}_2\text{O}_3$ to adsorb oxalic acid was much stronger than that of $\alpha\text{-FeOOH}$, and the adsorption of oxalic acid approached its maximum amount at about $C_{\text{ox}}^0 = 1.2 \text{ mM}$ on both iron oxides, which is consistent with the results of H_2O_2 formation in the present study. The detailed results of these adsorption experiments will be reported in another paper.

4. Conclusions

68% and 83% of PCP were photodegraded after 1 h reaction time at $C_{\text{ox}}^0 = 1.2 \text{ mM}$ in aqueous goethite and hematite suspensions, respectively. Dechlorination and detoxification (Microtox acute toxicity) of PCP were also achieved to a greater extent in the hematite suspension than in the goethite suspension, indi-

cating that hematite has the higher activity than goethite for PCP degradation in such an iron oxide-oxalate system under UVA illumination. The experiments further confirmed that more H_2O_2 could be formed in the hematite system than in the goethite system due to the more rapid iron cycling, which is beneficial to enhance the PCP degradation.

Acknowledgments

The authors appreciate the financial support by the National Science Foundation of China (No. 40771105).

References

- [1] M.E. Balmer, B. Sulzberger, Atrazine degradation in irradiated iron/Oxalate systems: effects of pH and oxalate, *Environ. Sci. Technol.* 33 (1999) 2418–2424.
- [2] Y.G. Zuo, J. Hoigne, Evidence for photochemical formation of H_2O_2 and oxidation of SO_2 in authentic fog water, *Science* 260 (1993) 71–73.
- [3] Y.G. Zuo, J. Hoigne, Formation of hydrogen peroxide and depletion of oxalic acid in atmospheric water by photolysis of iron(III)-oxalato complexes, *Environ. Sci. Technol.* 26 (1992) 1014–1022.
- [4] D. Papias, M. Taxiarchou, I. Douni, I. Paspaliaris, A. Kontopoulos, Thermodynamic analysis of the reactions of iron oxides: dissolution in oxalic acid, *Can. Metall. Quart.* 35 (1996) 363–373.
- [5] D. Papias, M. Taxiarchou, I. Paspaliaris, A. Kontopoulos, Mechanisms of dissolution of iron oxides in aqueous oxalic acid solutions, *Hydrometallurgy* 42 (1996) 257–265.
- [6] M.I. Litter, E.C. Baumgartner, G.A. Urrutla, M.A. Blesa, Photodissolution of iron oxides. 3. Interplay of photochemical and thermal processes in maghemite/carboxylic acid systems, *Environ. Sci. Technol.* 25 (1991) 1907–1913.
- [7] C. Siffert, B. Sulzberger, Light-Induced dissolution of hematite in the presence of oxalate: a case study, *Langmuir* 7 (1991) 1627–1634.
- [8] B. Sulzberger, H. Laubscher, Reactivity of various types of iron(III) (hydr)oxides towards light-induced dissolution, *Mar. Chem.* 50 (1995) 103–115.
- [9] P. Mazellier, B. Sulzberger, Diuron degradation in irradiated, heterogeneous iron/oxalate systems: The rate-determining step, *Environ. Sci. Technol.* 35 (2001) 3314–3320.
- [10] F.B. Li, X.Z. Li, X.M. Li, T.X. Liu, J. Dong, Heterogeneous photodegradation of bisphenol A with iron oxides and oxalate in aqueous solution, *J. Colloid Interface Sci.* 311 (2007) 481–490.
- [11] C.S. Liu, F.B. Li, X.M. Li, G. Zhang, Y.Q. Kuang, The effect of iron oxides and oxalate on the photodegradation of 2-mercaptobenzothiazole, *J. Mol. Catal. A-Chem.* 252 (2006) 40–48.
- [12] X.G. Wang, C.S. Liu, X.M. Li, F.B. Li, S.G. Zhou, Photodegradation of 2-mercaptobenzothiazole in the $\gamma\text{-Fe}_2\text{O}_3$ /oxalate suspension under UVA light irradiation, *J. Hazard. Mater.* 153 (2008) 426–433.
- [13] Q. Lan, F.B. Li, C.S. Liu, X.Z. Li, Heterogeneous Photodegradation of Pentachlorophenol with Maghemite and Oxalate under UVA Illumination, *Environ. Sci. Technol.* 42 (2008) 7918–7923.
- [14] D.L. Sedlak, J. Hoigne, The role of copper and oxalate in the redox cycling of iron in atmospheric waters, *Atmos. Environ.* 27A (1993) 2173–2185.
- [15] H. Liu, C. Wang, X. Li, X. Xuan, C. Jiang, H. Hui, A Novel electro-Fenton process for water treatment: reaction-controlled pH adjustment and performance assessment, *Environ. Sci. Technol.* 41 (2007) 2937–2942.
- [16] A. Safazadeh-Amiri, J.R. Bolton, S.R. Cater, Ferrioxalate-mediated photodegradation of organic pollutants in contaminated water, *Water Res.* 31 (1997) 787–798.
- [17] Y.G. Zuo, J. Zhan, Effects of oxalate on Fe-catalyzed photooxidation of dissolved sulfur dioxide in atmospheric water, *Atmos. Environ.* 39 (2005) 27–37.
- [18] B.C. Faust, R.G. Zepp, Photochemistry of aqueous iron(III)-polycarboxylate complexes: roles in the chemistry of atmospheric and surface waters, *Environ. Sci. Technol.* 27 (1993) 2517–2522.
- [19] J.S. Jeong, J.Y. Yoon, pH effect on OH radical production in photo/ferrioxalate system, *Water Res.* 39 (2005) 2893–2900.
- [20] F. Wu, N. Deng, Y. Zuo, Discoloration of dye solutions induced by solar photolysis of ferrioxalate in aqueous solutions, *Chemosphere* 39 (1999) 2079–2085.
- [21] X. Wang, L. Zhang, Y. Ni, J.H.X. Cao, Fast Preparation, characterization, and property study of $\alpha\text{-Fe}_2\text{O}_3$ nanoparticles via a simple solution-combusting method, *J. Phys. Chem. C* 113 (2009) 7003–7008.
- [22] J. Yu, X. Yu, B. Huang, X. Zhang, Y. Dai, Hydrothermal synthesis and visible-light photocatalytic activity of novel cage-like ferric oxide hollow spheres, *Cryst. Growth Des.* 9 (2009) 1474–1480.
- [23] J. Yu, G. Wang, B. Cheng, M. Zhou, Effects of hydrothermal temperature and time on the photocatalytic activity and microstructures of bimodal mesoporous TiO_2 powders, *Appl. Catal. B: Environ.* 69 (2007) 171–180.
- [24] M. Zhou, J. Yu, B. Cheng, Effects of Fe-doping on the photocatalytic activity of mesoporous TiO_2 powders prepared by an ultrasonic method, *J. Hazard. Mater.* 137 (2006) 1838–1847.
- [25] F.B. Li, X.Z. Li, C.S. Liu, T.X. Liu, Effect of alumina on photocatalytic activity of iron oxides for bisphenol A degradation, *J. Hazard. Mater.* 149 (2007) 199–207.
- [26] F.B. Li, X.G. Wang, Y.T. Li, C.S. Liu, F. Zeng, L.J. Zhang, M.D. Hao, H.D. Ruan, Enhancement of the reductive transformation of pentachlorophenol by polycarboxylic acids at the iron oxide-water interface, *J. Colloid Interface Sci.* 321 (2008) 332–341.
- [27] M.A. Oturan, N. Oturan, C. Lahitte, S. Trevin, Production of hydroxyl radicals by electrochemically assisted Fenton's reagent: Application to the mineralization of an organic micropollutant, pentachlorophenol, *J. Electroanal. Chem.* 507 (2001) 96–102.
- [28] M. Fukushima, K. Tatsumi, K. Morimoto, Influence of iron(III) and humic acid on the photodegradation of pentachlorophenol, *Environ. Toxicol. Chem.* 19 (2000) 1711–1716.
- [29] M. Fukushima, K. Tatsumi, Degradation pathways of pentachlorophenol by photo-Fenton systems in the presence of Iron(III), humic Acid, and hydrogen peroxide, *Environ. Sci. Technol.* 35 (2001) 1771–1778.
- [30] R.Z. Chen, J.J. Pignatello, Role of Quinone Intermediates as Electron Shuttles in Fenton and Photoassisted Fenton Oxidations of Aromatic Compounds, *Environ. Sci. Technol.* 31 (1997) 2399–2406.
- [31] F. Chen, W.H. Ma, J.J. He, J.C. Zhao, Fenton degradation of malachite green catalyzed by aromatic additives, *J. Phys. Chem. A* 106 (2002) 9485–9490.
- [32] R. Augusti, A.O. Dias, L.L. Rocha, R.M. Lago, Kinetics and mechanism of benzene derivative degradation with Fenton's reagent in aqueous medium studied by MIMS, *J. Phys. Chem. A* 102 (1998) 10723–10727.
- [33] R.W. Matthews, The reaction chemistry of aqueous ferrous sulfate solutions at natural pH, *Aust. J. Chem.* 36 (1983) 1305–1317.
- [34] T.E. Graedel, M.L. Mandich, Kinetic model studies of atmospheric droplet chemistry 2. Homogeneous transition metal chemistry in raindrops, *Geophys. Res.* 91 (1986) 5205–5221.
- [35] J. He, W.H. Ma, J.J. He, J.C. Zhao, J.C. Yu, Photooxidation of azo dye in aqueous dispersions of $\text{H}_2\text{O}_2/\alpha\text{-FeOOH}$, *Appl. Catal. B: Environ.* 39 (2002) 211–220.
- [36] S. Banwart, S. Davies, W. Stumm, The role of oxalate in accelerating the reductive dissolution of hematite ($\alpha\text{-Fe}_2\text{O}_3$) by ascorbate, *Colloid Surf.* 39 (1989) 303–309.